In-medium Spectral Functions in a Coarse-Graining Approach

Stephan Endres[1,2]**, Hendrik van Hees**[1,2]**, Janus Weil**[1,2] **and Marcus Bleicher**[1,2]

[1]Institut für Theoretische Physik, Universität Frankfurt, Max-von-Laue-Straße 1, 60438 Frankfurt, Germany
[2]Frankfurt Institute for Advanced Studies, Ruth-Moufang-Straße 1, 60438 Frankfurt, Germany

E-mail: `endres@th.physik.uni-frankfurt.de`

Abstract. We use a coarse-graining approach to extract local thermodynamic properties from simulations with a microscopic transport model by averaging over a large ensemble of events. Setting up a grid of small space-time cells and going into each cell's rest frame allows to determine baryon and energy density. With help of an equation of state we get the corresponding temperature T and baryon-chemical potential μ_{B}. These results are used for the calculation of the thermal dilepton yield. We apply and compare two different spectral functions for the ρ meson, firstly a calculation from hadronic many-body theory and secondly a calculation from experimental scattering amplitudes. The results obtained with our approach are compared to measurements of the NA60 Collaboration. A relatively good description of the data is achieved with both spectral functions. However, the hadronic many-body calculation is found to be closer to the experimental data with regard to the in-medium broadening of the spectral shape.

1. Introduction

Although it is widely accepted nowadays that the dynamics of strong interactions are governed by quantum chromodynamics (QCD), we still lack a full understanding of the QCD phase structure. At low energies and densities, the relevant degrees of freedom are hadrons, i.e., composite objects of quarks and gluons. However, for sufficiently large energies and/or densities the creation of a deconfined phase with free quarks and gluons is expected. Also the symmetry pattern of QCD is assumed to change - e.g., chiral symmetry which is broken in the vacuum but expected to be restored at some finite temperature. In consequence, the study of the in-medium properties of hadrons plays an important role especially for a better understanding of the non-perturbative part of QCD [1, 2]. Experimentally, heavy-ion collisions at ultra-relativistic energies are a good possibility to create hot and dense matter in the laboratory. However, the measurement of in-medium modifications is difficult, as the fireball has a lifetime of only a few fm/c, and all the hadronic observables only give information on the final freeze-out. Here dileptons offer the big advantage that they do not interact strongly and can leave the hot and dense fireball unscathed after their production. But this has a drawback, too. As lepton pairs are produced via many different processes at all stages of the reaction, their spectra reflect the whole evolution of the collision. What one can measure are only time integrated spectra. This is a challenge for theory, as it requires a reliable description of the entire reaction dynamics.

In these proceedings a coarse-graining approach [3] is used (following a similar ansatz as proposed by Huovinen et al. [4]), which allows to combine in-medium spectral functions with an underlying microscopic description of the reaction dynamics. We argue that this is a good and realistic compromise between transport approaches, where an inclusion of medium modifications of spectral functions is difficult, and fireball models that use a simplified description of the reaction evolution but where the application of spectral functions is straightforward. In contrast to common hydrodynamic models, its advantage is the unified description of the whole reaction dynamics, from the first hadron-hadron collisions to the final freeze-out (except for a different treatment of the very low temperature cells, see section 2).

2. The Model

The coarse-graining is based on the time-step-wise output from simulations with the Ultra-relativistic Quantum Molecular Dynamics model (UrQMD). It is a non-equilibrium transport approach and describes a nuclear reaction in terms of classically propagated hadrons combined with subsequent elastic and inelastic binary scatterings [5–7]. To extract thermodynamic properties, we take an ensemble of UrQMD events (≈ 1000) and average over them, such that we get a relatively smooth phase-space distribution function. Hereby the UrQMD output is set on a space-time grid with $\Delta t = 0.2$ fm/c and $\Delta x = 0.8$ fm. The choice of the cell size is a compromise between the highest possible resolution and the memory and computational requirements. However, we checked that a smaller size does not improve or change the results.

In each cell the baryon four-flow is then calculated and Eckart's definition [8] is used to perform a Lorentz boost into the local rest frame of the cell. This enables to calculate local baryon and energy densities. To extract the temperature T and baryon-chemical potential μ_B we use the equation of state of a hadron resonance gas [9] that includes the same hadronic degrees of freedom as the UrQMD model. To account also for dilepton emission from the quark-gluon plasma phase, we use a second equation of state for temperatures above 170 MeV that has been fitted to Lattice calculations [10]. As the values of T of the two EoS agree almost perfectly in the temperature range from 150 to 170 MeV, a smooth transition is guaranteed. Note, however, that the chemical potential is set to zero for $T > 170$ MeV, as the Lattice fit is only done for vanishing quark chemical potential. In consequence we can not have a smooth transition for μ_B. (Besides T and μ_B, we also calculate the effective baryon density, ρ_{eff}, in each cell, as it is the input for one of the spectral functions implemented here, see section 3 below). When we know the thermodynamic properties of the cell, the dilepton emission per four-volume and four-momentum is calculated according to [11]

$$\frac{\mathrm{d}N_{ll}}{\mathrm{d}^4x\mathrm{d}^4p} = -\frac{\alpha_{\mathrm{em}}^2}{\pi^3 M^2} L(M) f^{\mathrm{B}}(E;T) \operatorname{Im} \Pi_{\mathrm{em}}^{(\mathrm{ret})}(E,p;\mu_{\mathrm{B}},T) \tag{1}$$

with the dilepton phase-space function L and the Bose-distribution function f^{B}. In case of the thermal ρ emission the retarded electromagnetic current-current correlator is given by the in-medium propagator of the meson, $\operatorname{Im} \Pi_{\mathrm{em}} = (m_\rho^2/g_\rho)^2 \operatorname{Im} D_\rho$ (where m_ρ respectively g_ρ denote the bare mass and the coupling strength of the ρ).

Note that the original dilepton emission rate, as derived by McLerran and Toimela [12], assumes chemical equilibrium. However, here we use a generalization for an off-equilibrium situation with finite pion chemical potentials. In this case an additional squared fugacity factor $z_\pi^2 = \exp(2\mu_\pi/T)$ enters in equation (1) for the thermal ρ emission. Within our approach the pion chemical potential is extracted in each cell in the relativistic Boltzmann approximation. A positive value for μ_π means that the corresponding number of produced pions is larger than one would obtain in complete chemical equilibrium [13]. This is what we also find when using the input from the UrQMD model. As even small values of μ_π give a strong increase on the dilepton yield [14], it is important to include this effect in the calculations.

Although the focus is on the in-medium effects of the ρ in the present study, we need to consider also the other sources that contribute to the dilepton excess yield. For a full description one has to calculate the emission from the QGP, i.e., in our case for temperatures above 170 MeV. For this we use the rates from lattice calculations, which are extrapolated for finite momenta [15]. As we deal with extremely high densities of hadronic matter in the heavy-ion collisions under consideration, multi-pion interactions will also give a significant contribution for the dilepton yield. The rates used in our approach take vector-axialvector mixing into account [16, 17].

Finally, we have to consider the contribution from those cells, where the density (respectively temperature) is very low and therefore the assumption of a thermal emission is not reasonable. For these cells we simply take the ρ mesons from the UrQMD calculation directly and apply a shining procedure [18, 19]. As this is only done for the cells in which no thermal emission is considered, we avoid double counting.

For more details on the coarse-graining approach, the reader is referred to reference [3].

3. Spectral Functions

Only few approaches exist which model the influence of both finite temperature and baryon density on the ρ spectral function. We here apply and compare two widely used spectral functions: On the one hand, the hadronic many-body calculation by Rapp and Wambach (Rapp SF) [20] which has previously proven to be a good description of experimental results [11,16,17]. And secondly the more model-independent approach by Eletsky and others (Eletsky SF) [21] for which the self-energies of the ρ are calculated using empirical scattering amplitudes from resonance dominance. In the Rapp SF the propagator of the ρ takes the form

$$D_\rho(E,p) = \frac{1}{M^2 - M_\rho^2 - \Sigma_{\rho\pi\pi}(M) - \Sigma_{\rho M}(E,p) - \Sigma_{\rho B}(E,p)}, \qquad (2)$$

which includes interactions of the pion cloud with the ρ ($\Sigma_{\rho\pi\pi}$) and direct scatterings off mesons and baryons ($\Sigma_{\rho M}$, $\Sigma_{\rho B}$). The meson-gas effects include interactions with the most abundant π, K and ρ mesons and are saturated with resonances up to 1.3 GeV [20,22]. Similarly, the effects of the baryonic matter enter via direct $\rho N \to B$ scattering and resonance hole excitations [23,24]. For the Eletsky SF the ρ-meson self-energy is calculated within a heat bath of nucleons and pions. The in-medium modifications are then consequently determined by ρN and $\rho\pi$ scatterings. In the low-energy regime the calculation of the scattering amplitudes $f_{\rho a}(s)$ includes the resonances from the partial wave analysis by Manley [25], while at higher energies a Regge parametrization is applied. The contribution to the self-energy from the scattering of a ρ meson with a hadron is calculated in low-density expansion as

$$\Sigma_{\rho a}(E,p) = -4\pi \int \frac{\mathrm{d}^3 k}{(2\pi)^3} n_a(\omega) \frac{\sqrt{s}}{\omega} f_{\rho a}(s) \qquad (3)$$

with $\omega^2 = m_a^2 + k^2$ and the occupation number n_a. Note that in this model the scattering amplitudes are evaluated on the mass shell and therefore only depend on p here.

When comparing the two approaches for the spectral function, there are some caveats one has to consider. Especially it is important to know that the implementation of baryonic effects is not the same. In the parametrized version of the Rapp SF [26], which we use for our calculations, the baryonic effects enter via an effective baryon density $\rho_{\mathrm{eff}} = \rho_\mathrm{N} + \rho_{\bar{\mathrm{N}}} + 0.5 \left(\rho_{\mathrm{B}^*} + \rho_{\bar{\mathrm{B}}^*} \right)$. Firstly, this takes into account that the interaction of the ρ meson is the same with baryons and anti-baryons. And secondly it reflects the fact, that the scattering with excited baryons has less effect on the spectral shape [17]. As the Eletsky SF is determined for a gas of π and N only, not considering the effects of anti-baryons and excited resonance states, the baryon effects enter via a nucleon chemical potential μ_N. In the non-interacting hadron gas EoS, which we apply when determining
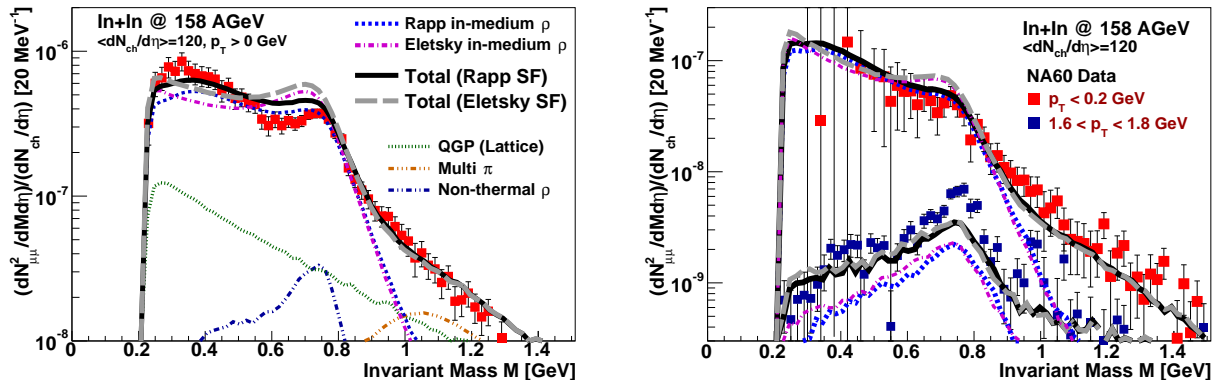
Figure 1. (Color online) Invariant mass spectra of the dilepton excess for In+In collisions at $E_{\mathrm{lab}} = 158\,A\mathrm{GeV}$ for the low-mass region for all p_t (left plot) and two distinct transverse momentum bins (right plot). The results are compared to the experimental data from the NA60 Collaboration [27–29].

T and μ_{B}, this μ_N is identical with the baryon-chemical potential μ_{B}. However, it is important to bear in mind that the degrees of freedom are different for the underlying UrQMD model and the hadron gas EoS on the one side and the πN gas, for which the scattering amplitudes of the Eletsky SF were calculated, on the other side. At SPS energies, a significant fraction of the baryons is found in an excited state in the UrQMD calculations, in conflict with the assumption of a gas of pions and nucleons only. Here a significantly higher degree of consistency is given with the hadron-resonance gas used for the hadronic many-body calculations by Rapp.

4. Results

The resulting invariant mass spectra from our coarse-graining calculation are presented in Figure 1. The left plot shows the total p_t-integrated yield. In general we achieve a rather good description of the measured spectra [27–29] with both spectral functions. A somewhat stronger melting of the peak at the ρ pole mass is however visible in case of the Rapp SF. It only slightly overshoots the NA60 data by about 20% in the mass range from 0.6 to 0.8 GeV, while the Eletsky SF gives a yield that is almost a factor of two above the data. This finding is in line with the fact that the Eletsky approach resembles a virial expansion, that is valid only for low densities. The broadening is mainly due to the presence of baryonic matter which in such heavy-ion collisions can easily reach several times normal matter density. Consequently it is clear that the low-density approximation will underestimate the effect. On the contrary, we get more dilepton yield in the mass range from 0.3 to 0.5 GeV with the Rapp SF, in better agreement with the data than the Eletsky SF. The latter additional enhancement was partly attributed to the inclusion of off-shell ρ-N resonances [2], whereas in the Eletsky SF the scattering amplitudes are calculated on-shell only. The overall shape of the invariant-mass spectrum is clearly better described when applying the Rapp SF; we find a stronger broadening here, in good agreement with the data. The other thermal dilepton sources, i.e., the quark-gluon plasma and the multi-pion interactions, only give relatively small contributions at low masses. However, they become significant in the mass range above 1 GeV, which is not considered in detail here. A relatively small contribution stems also from the non-thermal ρ.

In the right plot of Figure 1 we see the results for two transverse-momentum bins. The upper curves (with red data points) denote the results for $p_t < 0.2$ GeV, while the lower results (blue data points) are for momenta between 1.6 and 1.8 GeV. One can see from the comparison, that

the most dominant modification of the spectral functions is observed for low momenta. Here - as in the p_t-integrated spectrum - we find a stronger broadening for the Rapp SF, better describing the data around the pole mass. For the higher momentum window, the spectral shape of the ρ resembles more its vacuum shape. Consequently, the differences between the spectral functions become less dominant. However, for high p_t there remains some excess of the data above the model results around the ρ pole mass. Obviously we miss some of the "freeze-out" ρ contribution here. Note also that the thermal ρ contribution clearly dominates for invariant masses up to 1 GeV at low transverse momenta, while for the higher p_t bin it makes up only roughly 50% in this mass region, i.e., the QGP contribution and the non-thermal ρ become more relevant here (not shown in the plot for reasons of lucidity).

5. Summary & Conclusions

In general, the coarse-graining approach has proven its applicability for the description of experimental dilepton yields. Although the two spectral functions used in the present work stem from two rather different calculations, both give a reasonable description of the experimentally measured dilepton yields at SPS energy within the coarse-graining approach. In comparison, however, the description of the broadening (which is mainly due to scattering of the ρ with baryons) is more realistic in the hadronic many-body calculation by Rapp and Wambach.

References

[1] Leupold S, Metag V and Mosel U 2010 *Int. J. Mod. Phys. E* **19** 147–224
[2] Rapp R and Wambach J 2000 *Adv. Nucl. Phys.* **25** 1
[3] Endres S, van Hees H, Weil J and Bleicher M 2014 (*Preprint* arXiv:1412.1965 [nucl-th])
[4] Huovinen P, Belkacem M, Ellis P J and Kapusta J I 2002 *Phys. Rev. C* **66** 014903
[5] Bass S A, Belkacem M, Bleicher M, Brandstetter M, Bravina L *et al.* 1998 *Prog. Part. Nucl. Phys.* **41** 255–369
[6] Bleicher M, Zabrodin E, Spieles C, Bass S A, Ernst C *et al.* 1999 *J. Phys. G* **25** 1859–1896
[7] Petersen H, Bleicher M, Bass S A and Stöcker H 2008 (*Preprint* arXiv:0805.0567 [hep-ph])
[8] Eckart C 1940 *Phys. Rev.* **58** 919–924
[9] Zschiesche D, Schramm S, Schaffner-Bielich J, Stöcker H and Greiner W 2002 *Phys. Lett. B* **547** 7–14
[10] He M, Fries R J and Rapp R 2012 *Phys. Rev. C* **85** 044911
[11] Rapp R 2013 *Adv. High Energy Phys.* **2013** 148253
[12] McLerran L D and Toimela T 1985 *Phys. Rev. D* **31** 545
[13] Bandyopadhyay D, Gorenstein M, Stoecker H, Greiner W and Sorge H 1993 *Z. Phys. C* **58** 461–464
[14] Koch P 1992 *Phys. Lett. B* **288** 187–194
[15] Ding H T, Francis A, Kaczmarek O, Karsch F, Laermann E *et al.* 2011 *Phys. Rev. D* **83** 034504
[16] van Hees H and Rapp R 2006 *Phys. Rev. Lett.* **97** 102301
[17] van Hees H and Rapp R 2008 *Nucl. Phys. A* **806** 339–387
[18] Li G Q, Ko C M, Brown G E and Sorge H 1996 *Nucl. Phys. A* **611** 539–567
[19] Schmidt K, Santini E, Vogel S, Sturm C, Bleicher M *et al.* 2009 *Phys. Rev. C* **79** 064908
[20] Rapp R and Wambach J 1999 *Eur. Phys. J. A* **6** 415–420
[21] Eletsky V L, Belkacem M, Ellis P and Kapusta J I 2001 *Phys. Rev. C* **64** 035202
[22] Rapp R and Gale C 1999 *Phys. Rev. C* **60** 024903
[23] Rapp R, Urban M, Buballa M and Wambach J 1998 *Phys. Lett. B* **417** 1–6
[24] Urban M, Buballa M, Rapp R and Wambach J 1998 *Nucl. Phys. A* **641** 433–460
[25] Manley D and Saleski E 1992 *Phys. Rev. D* **45** 4002–4033
[26] Rapp R 2014 private communication
[27] Arnaldi R *et al.* (NA60 Collaboration) 2009 *Eur. Phys. J. C* **59** 607–623
[28] Specht H J (NA60 Collaboration) 2010 *AIP Conf. Proc.* **1322** 1–10
[29] Arnaldi R *et al.* (NA60 Collaboration) 2009 *Eur. Phys. J. C* **61** 711–720